A Luminescence Lifetime Imaging System Using Imaging Fibers to Measure the 2D Distribution of O_2 in Biological Samples

Gerhard Holst*[a], Björn Grunwald[a], Ingo Klimant[b] and Michael Kühl[c]

[a]Max-Planck-Institute for Marine Microbiology, Microsensor Research Group, Celsiusstr. 1, D-28359 Bremen, Germany
[b]Institute for Analytical Chemistry, Chemo- and Bio-Sensors, University of Regensburg, D-93040 Regensburg, Germany
[c]Marine Biological Laboratory, University of Copenhagen, Strandpromenaden 5, DK-3000 Helsingør, Denmark

Keywords: luminescence lifetime imaging, oxygen optode, planar optode, imaging fibers, endoscope, luminescence imaging

ABSTRACT

A new sensor head and imaging application with planar oxygen optodes is presented. It combines the versatility of the recently presented modular luminescence lifetime imaging system (MOLLI)[1] and the oxygen measuring features of planar optodes to investigate the 2D-distribution of oxygen with a high spatial resolution.
The marine sediments are settled by microorganisms. They are characterized by steep gradients of solutes perpendicular to the interface. Oxygen as the most favorable electron acceptor plays an important role in these communities and exhibits steep gradients within distances of 100 µm to a couple of millimeters. Traditionally these gradients are commonly accessed by either oxygen microelectrodes or oxygen microoptodes, that measure single oxygen depth profiles at spatial resolutions in the range of 50-5 µm. As the influences on the metabolism of these organisms are complex, profiles that are measured at one location exhibit a natural heterogeneity. To address this problem by using the potential of planar oxygen optodes first measurements with optodes fixed to an aquarium wall (Glud et al. 1996[14]) based on luminescence intensity measurements have been published. They showed the large amount of information that can be gathered by this method.
We further developed this approach by combining the planar optode with the capabilities of imaging fibers that form an endoscope. We developed a periscope type sensor head that can be independently applied in biological samples. It has an overall diameter of 2.5 mm and a calculated pixel resolution of 12 µm. The according measuring system compared to the published system[1] has a different excitation light setup and corresponding endoscope optics to measure the lifetime based images.
We present the adapted system, sensor head and the first results of an application.

1. INTRODUCTION

Imaging of two-dimensional (2D) solute distributions with luminescent indicators is now established as an important tool in medicine, biology and physics. Most of the described image measuring systems and experimental setups were designed for specific applications like measurements of oxygen distribution in tissue[2-5], pH and Ca^{2+} distributions in cells[6-9], oxygen partial pressure on skin surface or oxygen flux into skin[12, 13], oxygen distribution across the water-sediment interface[14, 16] and in biofilms[15]. These setups were optimized for the corresponding experimental situation, but most of them lack versatility and many of them were e.g. confined to microscope setups[7-9, 17-20]. Therefore we presented a new modular luminescence lifetime imaging system (MOLLI)[1] that should allow for a versatile application of the imaging system to various different applications. While many of the biological applications used the planar oxygen optode fixed to a transparent setup wall and sensors that consisted of non transparent sensing layers[14-16], we combined transparent sensing layers, which enable a structural investigation by just looking through the sensor to correlate the oxygen distribution with the sample behind, with imaging fibers, an industrial endoscope, to gain the free access within the sample.

* Correspondence: e-mail: gholst@mpi-bremen.de; WWW:http://www.mpi-bremen.de; Telephone: +49-(0)421-2028-834; Fax: +49-(0)421-2028-690

Part of the SPIE Conference on Fiber Optic Sensor Technology and Applications
Boston, Massachusetts • September 1999
SPIE Vol. 3860 • 0277-786X/99/$10.00

Endoscopes are commonly used for investigations in the human body in medicine or investigations in industrial applications which are not easy accessible. While there are few applications that use imaging fibers for measurement of parameter distributions at high spatial resolution[21-24], we combined the oxygen measuring features of planar optodes with the flexibility of imaging fibers to measure the oxygen distribution at a high spatial resolution. Here we describe a new application for MOLLI with an endoscope in the chosen setup configurations. It was possible to image a time series of the respiration of photosynthetically active cyanobacteria living in a symbiosis with a fungus as a lichen.

2. MATERIAL AND METHODS

2.1. Planar oxygen optode

The dynamic quenching of luminescence by oxygen is the basis for the measurement of oxygen concentrations and distributions in various systems[1, 2-5, 12, 13, 14-16, 27-31]. The applied sensors have a planar structure with the luminescent indicator embedded in PVC that is spread by a knife coating process on a transparent polyester support foil (Mylar, DuPont, USA). The applied indicator, ruthenium(II)-tris-4,7-diphenyl-1,10 phenantroline perchlorate ($Ru[diph]_3$), is widely used for oxygen measuring purposes. It has a high quantum yield, long decay or lifetimes and its absorption spectrum nearly perfectly overlaps with the emission spectrum of blue LED's and its large Stokes shift with the emission maximum at 605 nm makes it very suitable for luminescence lifetime imaging[1, 12, 13]. The sensor area is imaged through the endoscope and an optical emission filter onto the CCD chip of the camera. each pixel now monitors the light intensity of the luminescence light emission, or, with proper timing, a part of the decay curve.
We calibrate the oxygen optodes with a two component model of the Stern-Volmer equation, that was derived and experimentally modified from a two component model published by Carraway et al. 1991[25, 26]:

$$\frac{\tau}{\tau_0} = \frac{I}{I_0} = \frac{frac}{(1 - K_{sv} \cdot [O_2])} + (1 - frac)$$

with τ_0, τ - lifetime in the absence of oxygen or with oxygen, I_0, I - luminescence intensity in the absence or with oxygen, K_{sv} - bimolecular quenching coefficient, $[O_2]$ - oxygen concentration in % volume or % air saturation, frac - fractionating factor.

2.2. Endoscope

The first approach was to use the smallest available industrial version of an endoscope, consisting of 10000 imaging fibers and a fiber ring for illumination build in a stainless steel capillary of an overall diameter of 1.5 mm. The fibers had a length of 1.5m and the maximum achievable resolution was appr. 11 µm per fiber (working distance 2 mm).

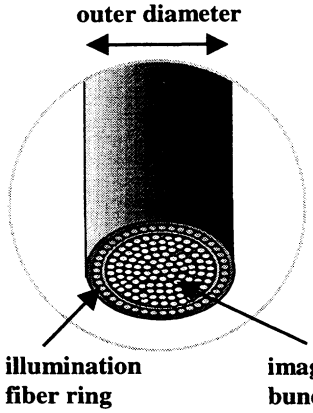

	tested version	*planned version*
diameter inner (outer)	**0.91 mm (2 mm)**	***0.91 mm (2 mm)***
imaging fibers	**30000**	***30000***
view angle	**71°**	***45°***
working distance	**4 mm**	***2.5 mm***
resolution:		
at surface	**5 µm / fiber**	***5 µm / fiber***
2.2 mm distance	**24 µm / fiber**	***16 µm / fiber***
4.2 mm distance	**40 µm / fiber**	***25 µm / fiber***

Figure 1: Characteristical data of the used endoscope:
The tested version column depicts the endoscope that was used in the application, while the second column shows the data of the endoscope that will be used for futural applications

This endoscope should be coupled to a 45° prism to enable imaging perpendicularly to the direction of fiber penetration in a sample (Fig. 2 [a]). Unfortunately we could not get enough light out of it, unless we used a binning of 8 pixels, which reduces the resolution by a factor of 4. So we decided to try experiments with a larger standard endoscope (described in figure 1, Schölly Fiberoptic, Denzlingen, Germany). Because we got this endoscope to test, additional parameters are given in the table (Fig. 1, 2nd column) to show the values of a version that is currently under construction. The overall diameter of 2 mm was still acceptable while the large view angle of 71° caused problems with sharpening of the black & white image. Here the depth of information was not very clear, but the lifetime images were restricted to the layer where the luminescence was generated.
The principle of these industrial endoscopes is simple, the core bundle consists of imaging fibers with diameters of 4-5 µm. With additional imaging optics at both ends the image is transferred to the CCD chip in the camera, the connection is a standard C-mount. Around the imaging fibers there is a ring of illumination fibers, where a side incoupling at the camera end of the endoscope, enables the coupling of illumination light, that either could be from a white light source or for luminescence measurements from blue LED's.

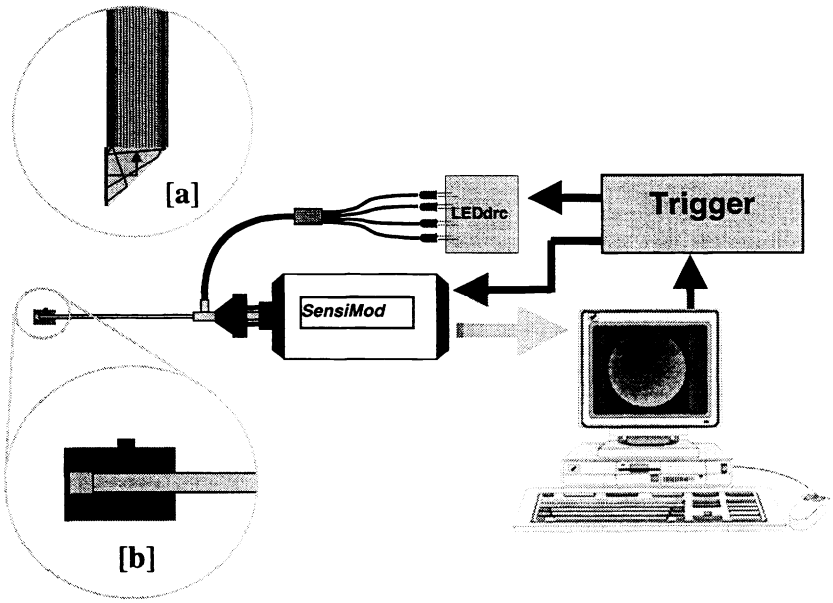

Figure 2: MOLLI system with endoscope application - the PC controls the trigger source (Trigger) and receives the digital images from the CCD-camera (SensiMod). The trigger source, a pulse delay generator generates the timing signals that control the excitation light source (4 LED's, λ_{peak}=470nm, that are driven by a special driving circuit, LEDdrc) and the electronic shutter of the camera. The planned periscope setup [a] will allow for measurements perpendicular to the penetration direction, while the presented results are obtained with a butted end [b] setup.

As the planned inverse periscope setup (Fig. 2 [a]) could not be used with the tested endoscope we realized a butted end version (Fig.2 [b]) where an optode holder was mounted on top of the endoscope. Between the endoscope and the planar optode is a 2 mm thick polycarbonate distance window to generate the necessary working distance.

2.3. MOLLI - Imaging system

The imaging system (Fig. 2), MOLLI, consists of an electrically cooled CCD-camera (SensiMod, PCO Computer Optics, Kehlheim, Germany) with a direct fast electronical shutter feature. Additionally the camera has a special customized modulation input to control directly the fast shutter (t_{on} = 500 ns and t_{off} = 500 ns, maximum modulation frequency 1 MHz). The camera (dynamic range 12 = Bit, resolution 640x480 pixel) is connected via a serial fiberoptical link to a camera control PCI-board in a Pentium based PC (Fig. 2). The PC controls image acquisition, storage, display and the timing.. For the precise timing of excitation light source switching and image acquisition, The PC is connected via a standard GPIB interface to a pulse delay generator (Fig.2, trigger, DG535, SRS Stanford Research Systems, Sunnyvale, USA). Timing control and primary image

acquisition was programmed in Delphi 4 (Delphi 4, Borland, Scotts Valley, USA), while the image processing and visualization were programmed in IDL 5.2 (Research Systems Inc., Boulder, USA).
The camera was connected to the industrial endoscope that is described above. The excitation light source consists of 4 LED's (HLMP-CB15, Hewlett Packard, USA) coupled into a fiber bundle that is connected to the illumination light input of the endoscope. The LED's are driven by a self developed driving circuit (Fig. 2, LEDdrc) that is connected to the pulse delay generator.

2.4. Timing of image acquisition

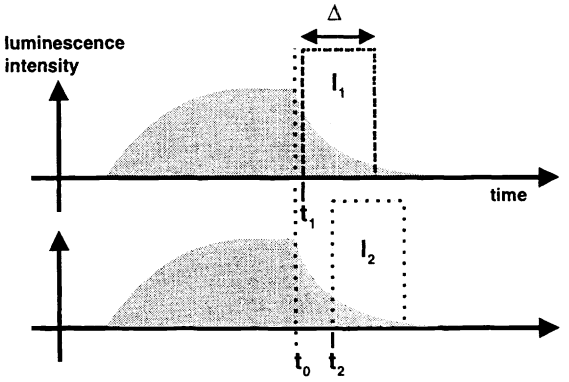

Figure 3: Principle image acquisition timing scheme for luminescence lifetime imaging. The given luminescence signal vs. time corresponds to the light signal that is detected by each pixel of the CCD-chip. The timing starts with excitation light ON and the camera shutter closed, the luminophore absorbs light and luminescence is emitted. Then the excitation light is switched OFF and the camera shutter is opened. This is repeated numerous times during the overall camera "integration" time.

Figure 3 shows the detection principle that is applied for each pixel. First the excitation light source is switched ON e.g. for 4 µs and illuminates the planar optode. The luminescence that is detected by each pixel rises until an equilibrium between absorbed and emitted energy of the dye molecules is reached (Fig. 3, time course of the luminescence signal). Then the light source is switched OFF and appr. 0.5 µs later the camera shutter is opened allowing ambient light and luminescence to reach the CCD chip for a certain time window e.g. 3 µs. This is repeated for a number of times, while the incident light is integrated on the CCD chip before the image is passed to the PC. For further improvement of the signal to noise ratio, the procedure can be repeated a couple of times to perform an efficient averaging. Additionally the image detection is repeated without the excitation light being switched ON to record a background or dark image, that directly can be subtracted from the measured images to prevent the ambient light information in the images from being further processed.

2.5. Evaluation of lifetime images

To evaluate the corresponding lifetime of the light information detected by each pixel, two sets of images are collected, where each set is acquired with a different delay time t_i relative to the switch OFF event of the excitation light source (Fig. 4).
The basic assumption is that the decay curve follows a monoexponential decay. Many investigations have shown that in principle 4 or even more lifetimes can be fitted to a recorded decay curve of such a sensor, while for practical sensing applications; the use of a single so called apparent lifetime seems to be justified (as can be seen by the comparison of raw data and model fit in figure 7).
The following image processing procedure is performed. Two sets of images (i = 1,2) are collected (Fig. 4), while each image detection with a time interval Δ_i has a certain delay t_i compared to the excitation light OFF event. To receive enough light intensity each image represents the integral over a number, n_i, of illumination events. The measured images S_i are stored after subtracting the dark image. The intensity of one image is given by:

$$I_i = \frac{S_i}{n_i}, i = 1,2$$

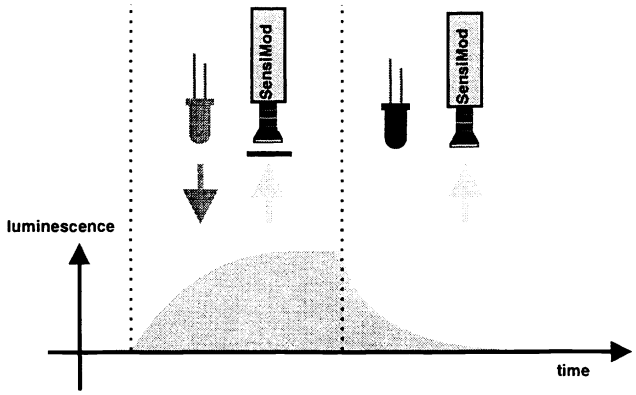

Figure 4: Timing scheme for recording of images to calculate the corresponding lifetime images. All detected images have the same width Δ and integrate the intensity I_i of the decay curve. Each window has a different delay t_i compared to the switch OFF time of the excitation light. The window "open" operation is repeated several times for the same delay t_i to integrate the light information on the CCD chip.

This intensity is, assuming a monoexponential decay curve with the apparent lifetime τ, described by the following equation:

$$I_i = I_0 \cdot \tau \cdot \exp\left(\frac{t_i}{\tau}\right) \cdot \left[1 - \exp\left(-\frac{\Delta_i}{\tau}\right)\right]$$

with the unknown intensity I_0 at the time t_0 when the excitation light is switched OFF. As the image collection uses a constant detection window width:

$$\Delta_1 = \Delta_2 = \Delta$$

The further image processing is reduced to:

$$\tau = \frac{\Delta}{\ln(S_1/S_2)}$$

If the further reduction of noise is necessary, it is possible to increase the number of windows and average the lifetime results, but in our applications the 2 window approach was sufficient.

3. EXPERIMENTAL SETUP & RESULTS

3.1 Experimental setups

3.1.1. Calibration measurements

To check the homogeneity of the prepared planar optodes and the performance of the optical setup calibration measurements with a specific setup (Fig. 5, [a]) were made. The CCD-camera with the endoscope was attached to a flow through cell, that could be perfused with defined gas mixtures. The gas mixtures of oxygen and nitrogen were generated by a gas mixing pump (Wösthoff, Bochum, Germany), that allowed for mixtures with a precision of 0.1 % of the adjusted value. The gas was pumped against a constant water level of 150 mm. Inside the cell the a piece of the transparent planar optode was mounted and sets of images were taken at the following oxygen concentrations: 0 – 5 – 10 – 20 – 30 – 50 – 70 – 100 % volume of oxygen. The images were measured at a binning of 4, which result in a resolution of 350 µm per pixel. Later these image sets were used to calculate the corresponding lifetime images that can be seen in figure 6. To compare the results with the assumed two

component model, a region of interest, which covered appr. 90% of the whole endoscope image, was cut out in each lifetime image and used for a mean and standard deviation calculation. The results are given as numbers below each image in figure 6 and as a graph in figure 7. These average values were also used to determine a fit to the model with the three variables: lifetime at zero oxygen, t_0, quenching coefficient, K_{sv}, and the fraction factor, frac. The result is shown in figure 7.

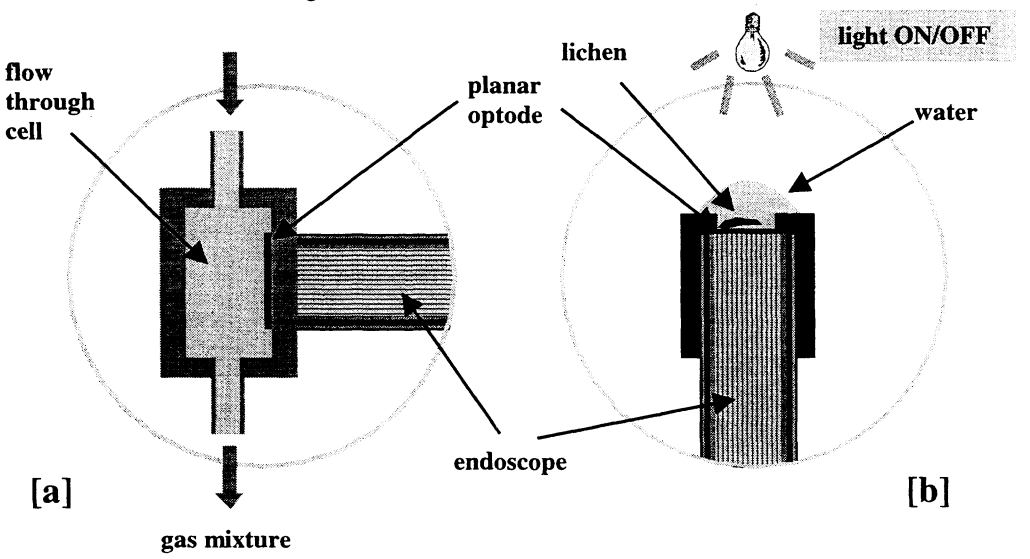

Figure 5: Experimental setups for measurements with the endoscope:
[a] The endoscope is attached to a flow through cell, in which the transparent planar optode is attached to a 3 mm thick glass plate inside the cell. Different gas mixtures of oxygen and nitrogen are perfusing the cell during the measurement.
[b] A piece of lichen is placed on top of the transparent planar optode, that is separated from the endoscope (not shown) by a 2mm thick polycarbonate window. Then this configuration is covered with a large water drop (diameter appr. 5 mm).

3.1.2. Oxygen consumption of cyanobacteria in a lichen

The camera was turned upward and a special optode holder was fixed on top of the endoscope. A dry piece of the soil lichen *Collema sp.* (Utah, USA), that is a symbiosis of a fungus and the cyanobacterium *Nostoc* was put on top of the optode. Then a large water drop was placed to cover the lichen and the optode (Fig. 5, [b]). The whole setup was illuminated by a halogen lamp for appr. 30 minutes. The light was switched off and appr. every minute image sets were taken for 20 minutes. Then a black & white image was recorded by using the white light as illumination. Finally water and lichen were removed and two calibration images were recorded, one with an air saturated and one with deaerated water drop. These were used to generate the K_{sv} image, which is together with the zero oxygen lifetime image necessary to convert the measured images into images of the oxygen distribution. All images except the black & white one, which was measured without binning (corresponds to 16.2 µm per pixel resolution), were measured with a binning of 2, which according to the distance of the optode from the endoscope surface results in a resolution of appr. 65 µm per pixel.

3.2. Results

3.2.1. Calibration measurements

As the images in figure 6 are scaled to the maximum lifetime value which is set to the maximum gray level (white = 255), the gray level in the images nicely reflect the hyperbolic relation between the lifetime values and the oxygen concentration. In the range between 0 and 20 % oxygen there is a large dynamic of 2.816 µs from τ_0 = 5.046 µs to τ = 2.23 µs while the lifetime change from 20 % to 100 % oxygen amounts to 1.059 µs.

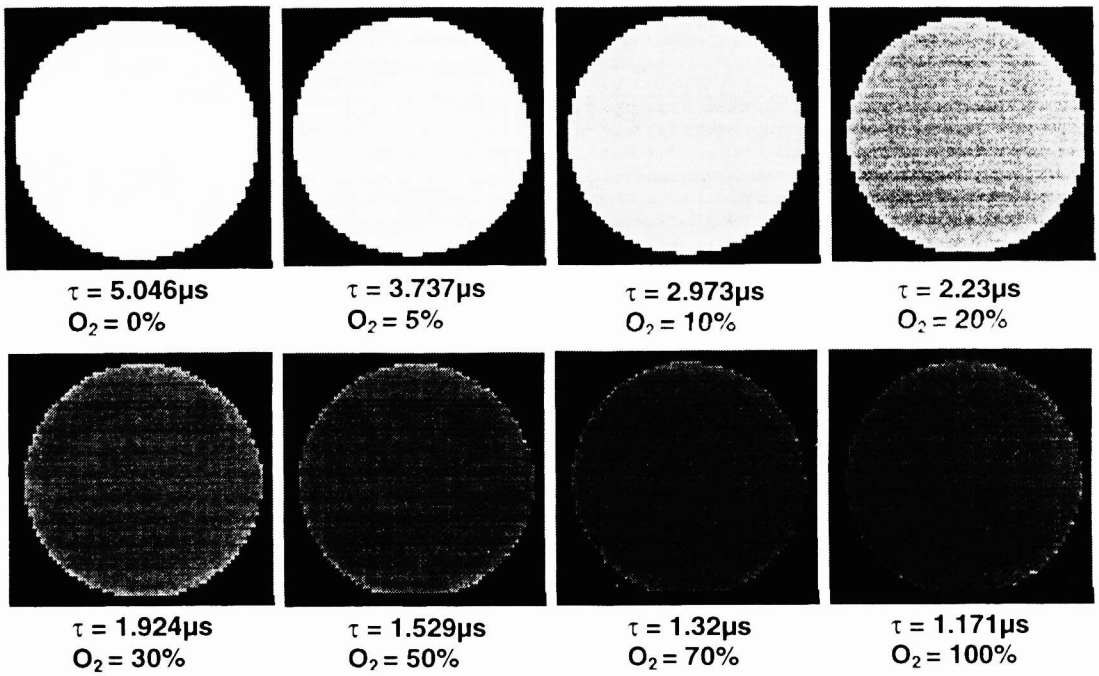

Figure 6: Luminescence lifetime images obtained with the endoscope in the calibration measurement setup. Each image corresponds to a different oxygen/nitrogen mixture present in the flow through cell. Below the images the oxygen concentration in percent volume oxygen and the average apparent lifetime is given (has been averaged about 90% of the endoscope image).

Furthermore the result of fitting the model to the raw average lifetime data demonstrates the quality of the model to describe the characteristics of the sensor and the good agreement of the assumption of an apparent lifetime to describe real world data. The practical approach of considering the fraction factor as constant = 0.85 seems to be justified. The following table gives the fit values:

lifetime at zero oxygen τ_0	**5.0545 µs**
quenching coefficient K_{sv}	**0.0916 %$^{-1}$**
fraction factor frac	**0.8523**
correlation r	**0.999535**

3.2.2. Oxygen consumption of cyanobacteria in a lichen

If the desert lichens *Collema sp.* (Utah, USA) are covered with water and illuminated with light the cyanobacteria *Nostoc* that live in this symbiosis start their photosynthetic activity. As the samples were illuminated for more than 30 minutes the cyanobacteria oversaturated the water drop with their oxygen production, because they produce more oxygen than they consume. When the illumination is switched OFF, there is only respiration, so oxygen is consumed which can nicely be followed by the changing oxygen distributions in the time series in figure 8. While the water drop becomes more and more oxygen depleted, it can be seen that the lichen was touching in the upper part of the image the sensing foil because the decrease on oxygen is here the fastest and deepest compared to the whole image. This is something that cannot be seen from the black and white image because of the large view angle of this endoscope of 71° (anything from the working distance to infinity is displayed sharp).

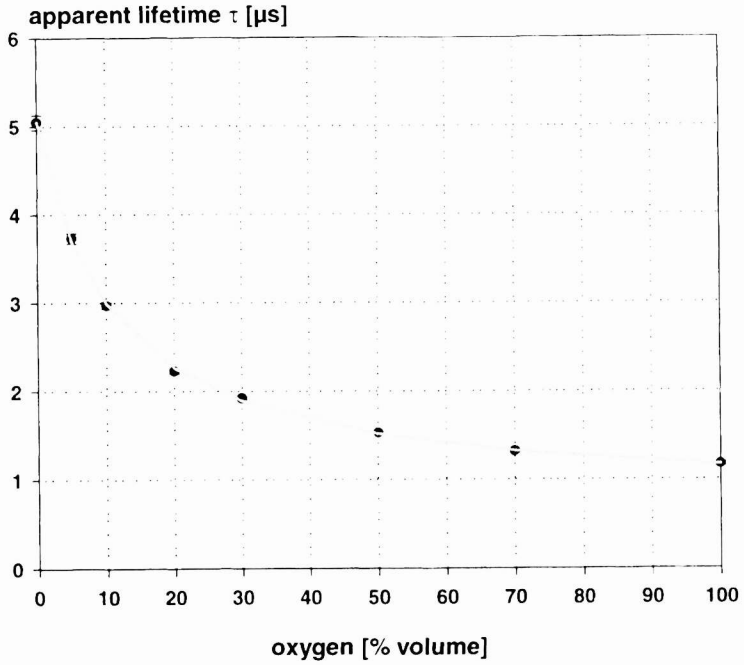

Figure 7: Comparison of average lifetime data from endoscope measurements (see figure 6) with fit of the applied model: raw data - black circles and error bars, fit curve - gray curve (fit values are given in the table above).

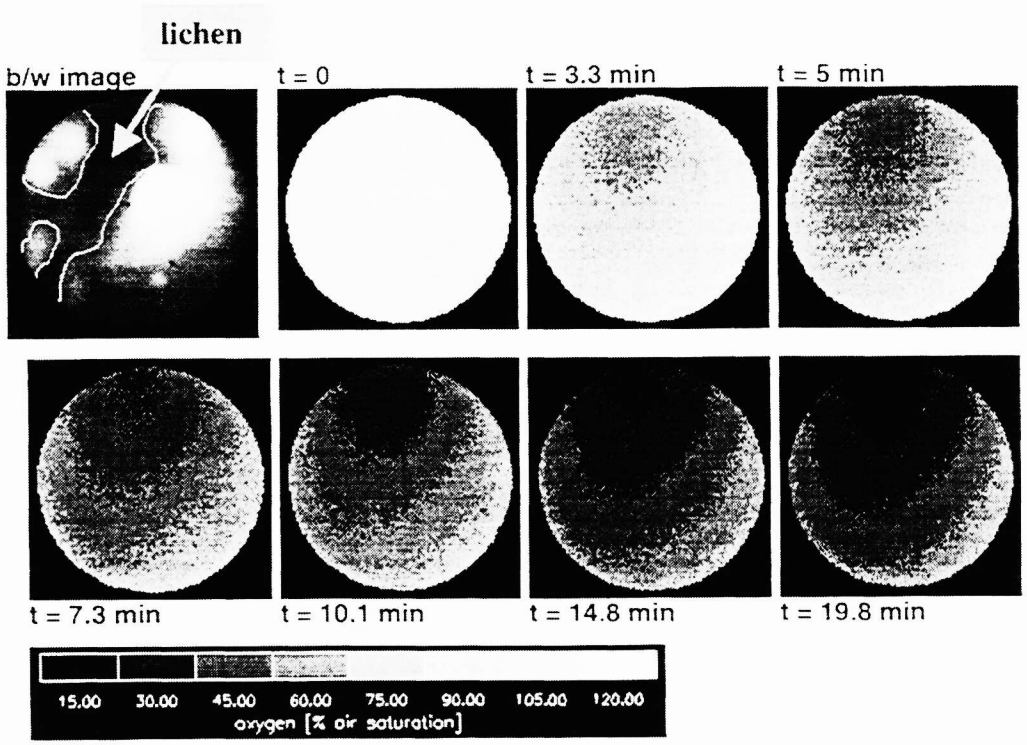

Figure 8: Black & white image of the lichen in front of the endoscope and time series of oxygen images, that was started after 30 minutes of illumination and 1 minute switching off the light. Each image was measured at a certain time after start of the darkness, reflecting the respiration of the cyanobacteria, that while being illuminated have produced oxygen and consume oxygen in the darkness. The gray level bar gives the coding in percent air saturation (100 % air saturation corresponds to appr. 20 % volume oxygen.

4. DISCUSSION

Although the originally planned application with a small endoscope have not yet been achieved, the presented results using a little larger endoscope (outer diameter 2 mm and 30000 imaging fibers) demonstrate that such an endoscope is a useful application of the modular luminescence lifetime imaging system MOLLI. With a further optimization step concerning smaller view angle and working distance, leading to a more distinct imaged distance the projected spatial resolution of 15 µm can be achieved.

The calibration measurements proved that for the first time both, the measurement of the 2D oxygen distribution, and a structural analysis, can be achieved almost simultaneously. Before this only was possible by some procedural tricks such as the application of dithionate grains to the sample to visualize the surface by measuring the oxygen change. The only drawback of the PVC sensors, that have such a high quantum efficiency and dynamic, is the overall lifetime of the sensor. The sensor changes its calibration characteristics with the evaporation of the PVC solvent, which results in 4-5 days application without recalibration. But this might be handled with a organically modified sol-gel as immobilization matrix with reduced dynamic but a lifetime of months. The choice mostly depends on the planned application.

The measurement of the oxygen respiration of a lichen nicely shows how fast and efficient these organisms change the oxic conditions in their nearby environment. This could be only weakly measured with single microsensors. Here, the imaging technique can give much more insight in the physiological conditions of these organisms. Therefore the endoscope application of MOLLI should allow enhanced investigation possibilities in biological research.

ACKNOWLEDGEMENTS

The authors would like to acknowledge the technical help with the camera system of M. Blaschke (PCO Computer Optics, Kehlheim, Germany) and the technical help of W. Glatz with IDL programming (Creaso, Gilching, Germany). Furthermore F. Garcia-Pichel is thanked for the lichen sample and valuable discussions about the interpretation of the results. Finally the Max-Planck-Society is thanked for financial support.

REFERENCES

1. G. Holst, O. Kohls, I. Klimant, B. König, M. Kühl, and T. Richter, "A modular luminescence lifetime imaging system for mapping oxygen distribution in biological samples", *Sensors and Actuators B* **51**, pp. 163-170, 1998.
2. W.L. Rumsey, J.M. Vanderkooi, and D.F. Wilson, "Imaging of Phosphorescence: a Novel Method for Measuring Oxygen Distribution in Perfused Tissue", *Science* **241**, pp. 1649-1651, 1988.
3. W.L. Rumsey, R. Iturriaga, D.F. Wilson, S. Lahiri, and D. Spergel, "Phosphorescence and Fluorescence Imaging: New Tools for the Study of Carotid Body Function", in *Chemoreceptors and Chemoreceptor Reflexes*, pp. 73-79, Plenum Press, New York, 1990.
4. R.D. Shonat, D.F. Wilson, C.E. Riva, and M. Pawlowski, "Oxygen Distribution in the Retinal and Choroidal Vessels in the Cat as Measured by a New Phosphorescence Imaging Method", *Appl. Opt.* **31**, pp. 3711-3718, 1992.
5. S. Vinogradov, L.-W. Lo, W.T. Jenkins, S.M. Evans, C. Koch, and D.F. Wilson, "Noninvasive Imaging of the Distribution in Oxygen in Tissue In Vivo Using Near-Infrared Phosphors", *Biophys. J.* **70**, pp. 1609-1617, 1996.
6. S. Nomura, M. Nakao, T. Nakanishi, S. Takamastu, and K. Tomita, "Real Time Imaging of Microscopic pH Distribution with a Two-Dimensional pH-Imaging Apparatus", *Anal. Chem.* **69**, pp. 977-981, 1997.
7. J.R. Lakowicz and K.W. Berndt, "Lifetime-Selective Fluorescence Imaging Using a RF Phase Sensitive Camera", *Rev. Sci. Instrum.* **62**, pp. 1727-1734, 1991.
8. J.R. Lakowicz, "Fluorescence Lifetime Imaging Sensing Generates Cellular Images", *Laser Focus World* **5**, 1992.
9. J.R. Lakowicz, H. Szmacinski, K. Nowaczyk, K.W. Berndt, and M. Johnson, "Fluorescence Lifetime Imaging", *Anal. Biochem.* **202**, pp. 316-330, 1991.
10. A.A. Panova, P. Pantano, and D.R. Walt, "In Situ Fluorescence Imaging of Localized Corrosion with a pH-Sensitive Imaging Fiber", *Anal. Chem.* **69**, 8, pp. 1635-1641, 1997.
11. P. Pantano and D.R. Walt, "Analytical Applications of Optical Imaging Fibers", *Anal. Chem.* **67**, pp. 481A-487A, 1995.

12. P. Hartmann and W. Ziegler, "Lifetime Imaging of Luminescent Oxygen Sensors Based on All-Solid-State Technology", *Anal. Chem.* **68**, pp. 4512-4514, 1996.
13. P. Hartmann, W. Ziegler, G. Holst, and D.W. Lübbers, "Oxygen Flux Fluorescence Lifetime Imaging", *Sensors and Actuators B* **38-39**, pp. 110-115, 1997.
14. R.N. Glud, N.B. Ramsing, J.K. Gundersen, and I. Klimant, "Planar Optrodes: A New Tool for Fine Scale Measurements of Two-Dimensional O_2 Distribution in Benthic Communities", *Mar. Ecol. Prog. Ser.* **140**, pp. 217-226, 1996.
15. R.N. Glud, C.M. Santegoeds, D. DeBeer, O. Kohls, and N.B. Ramsing, " Oxygen Dynamics at the Base of a Biofilm Studied with Planar Optodes, *Aquat. Microb. Ecol.* **14**, pp. 223-233, 1998.
16. R.N. Glud, M. Kühl, O. Kohls, and N.B. Ramsing, "Heterogeneity of Oxygen Production and Consumption in a Photosynthetic Microbial Mat as Studied by Planar Optodes", *J. Phycol.* **35**, pp. 270-279, 1999.
17. C.G. Morgan, A.C. Mitchell, and J.G. Murray, "Fluorescence Decay Time Imaging Using an Imaging Photon Detector with a Radiofrequency Photon Correlation System", in *Conference on Time-Resolved Laser Spectroscopy in Biochemistry II, Proc. SPIE*, pp. 798-807, 1990.
18. G. Marriott, R.M. Clegg, D.J. Arndt-Jovin, and T.M. Jovin, "Time Resolved Imaging Microscopy", *Biophys. J.* **60**, pp. 1374-1387, 1991.
19. R.M. Clegg, B. Feddersen, E. Gratton, and T.M. Jovin, "Time Resolved Imaging Fluorescence Microscopy", *Conference on Time-Resolved Laser Spectroscopy in Biochemistry II, Proc. SPIE*, pp. 448-460, 1990.
20. X.F. Wang, T. Uchida, D.M. Coleman, and S. Minami, "A Two-Dimensional Fluorescence Lifetime Imaging System Using a Gated Image Intensifier", *Appl. Spec.* **45**, pp. 360-366, 1991.
21. J.C. Carter, W.J. Egan, R.B. Nair, C.J. Murphy, S.L. Morgan, and S.M. Angel, "Fiber-Optic Imaging for In-Situ Chemical Measurements", *Proc. SPIE* **3540**, pp. 210-221, 1998.
22. S.J. Glenn, B.M. Cullum, J.C. Carter, R.B. Nair, D.A. Nivens, C.M. Murphy, and S.M. Angel, "Development of a Lifetime-Based Fiber-Optic Imaging Sensor to Study Water Transport in Thin Nafion™ Membranes", *Proc. SPIE* **3540**, pp. 235-245, 1998.
23. H.T. Skinner, T.F. Cooney, S.K. Sharma, and S.M. Angel, "Remote Raman Microimaging Using an AOTF and a Spatially Coherent Microfiber Optical Probe", *Appl. Spectroscop.* **50**, 8, pp. 1007-1013, 1996.
24. K.S. Bronk, K.L. Michael, P. Pantano, and D.R. Walt, "Combined Imaging and Chemical Sensing Using a Single Optical Imaging Fiber", *Anal. Chem.* **67**, 17, pp. 2570-2757, 1995.
25. E.R. Carraway, J.N. Demas, B.A. DeGraff, and J.R. Bacon, "Photophysics and Photochemistry of Oxygen Sensors Based on Luminescent Transition-Metal Complexes", *Analytical Chemistry* **63**, pp. 337-342, 1991.
26. E.R. Carraway, J.N. Demas, and B.A. DeGraff, "Luminescence Quenching Mechanism for Microheterogeneous Systems", *Analytical Chemistry* **63**, pp. 332-336, 1991.
27. G. Holst, M. Kühl, and I. Klimant, "A Novel Measuring System for Oxygen Microoptodes based on Phase Modulation Technique", *Proc. SPIE* **2508**, pp. 387-398, 1995.
28. I. Klimant, P. Belser, and O.S. Wolfbeis, "Novel Longwave Absorbing and Emitting Transition Metal Complexes for Use in Optical Oxygen Sensing", *Europt(r)ode I, Graz, 1,* 1992.
29. I. Klimant, V. Meyer, and M. Kühl, "Fiber-Optic Oxygen Microsensors, a New Tool in Aquatic Biology", *Limnology & Oceanography* **40**, pp. 1159-1165, 1995.
30. I. Klimant, G. Holst, and M. Kühl, "Oxygen Microoptodes and their Application in Aquatic Environment", *Proc. SPIE* **2508**, pp. 375-386, 1995.
31. I. Klimant, M. Kühl, R.N. Glud, and G. Holst, "Optical Measurement of Oxygen and Temperature in Microscale: Strategies and Biological Applications", *Sensors and Actuators B* **38**, pp. 29-37, 1997.